Identification and Characterization of ERK MAP Kinase Phosphorylation Sites in Smad3[†]

Isao Matsuura,[‡,§,||,⊥] Guannan Wang,[‡,§,||,⊥,▽] Dongming He,[§,||,⊥] and Fang Liu*[,§,||,⊥,▽]

Center for Advanced Biotechnology and Medicine, Susan Lehman Cullman Laboratory for Cancer Research, Department of Chemical Biology, Ernest Mario School of Pharmacy, Cancer Institute of New Jersey, and Graduate Program in Molecular Biology and Biochemistry, Rutgers, The State University of New Jersey, 679 Hoes Lane, Piscataway, New Jersey 08854

Received March 28, 2005; Revised Manuscript Received July 11, 2005

ABSTRACT: Smad3 is phosphorylated by ERK MAP kinase upon EGF treatment. We have mapped the ERK phosphorylation sites to Ser 207, Ser 203, and Thr 178 in Smad3. We show that, upon EGF treatment, Smad3 is rapidly phosphorylated in these sites, peaking at ∼15−30 min and that MEK1 inhibitors PD98059 and U0216 inhibit Smad3 phosphorylation induced by EGF. Ser 207 is the best ERK site in Smad3. Its phosphorylation shows the highest EGF induction in Smad3. It is also a very sensitive site to EGF treatment, significantly responding to low concentrations of EGF. These three sites are also phosphorylated by recombinant ERK2 in vitro. We have compared the kinetic parameters of Smad3 with those of ELK1 and MBP for ERK2. We further show that mutation of the ERK phosphorylation sites increases the ability of Smad3 to stimulate a Smad target gene, suggesting that ERK phosphorylation inhibits Smad3 activity.

TGF-β[1] family members regulate a wide variety of biological responses (*1*). Smad proteins can transduce the TGF-β signal at the cell surface into gene regulation in the nucleus (*2*−*7*). The Smad family is divided into different groups (*2*−*7*). One group includes the pathway-specific Smads, also referred to as R-Smads, which are phosphorylated by receptor kinases. For example, Smad2 and Smad3 are phosphorylated by the TGF-β receptor kinase in the C-terminal tail. The second group consists of the Co-Smads, which are commonly used in various TGF-β family members signaling pathways. Smad4 is the only member of this group in vertebrates. Upon TGF-β treatment, Smad2 and Smad3 are phosphorylated by the TGF-β receptor, form complexes with Smad4, and together accumulate in the nucleus. Often in conjunction with DNA-binding factors, Smads regulate transcription of responsive genes (*2*−*7*).

Smad activity is also regulated by phosphorylation through nonreceptor kinases. Smads contain a proline-rich region, termed the linker region, which connects the conserved N-terminal and C-terminal domains. The linker region is divergent in sequence and in length among Smads (*2*−*7*). The linker regions of R-Smads contain demonstrated, as well as suspected, phosphorylation sites for proline-directed kinases, such as ERK MAP kinase, c-Jun N-terminal kinase, p38 MAPK, cyclin-dependent kinases, as well as other kinases, such as Ca^{2+}-calmodulin-dependent kinase II (*8*−*25*). For example, we have mapped the CDK phosphorylation sites to Thr 8, Thr 178, and Ser 212 in Smad3, and we have shown that CDK phosphorylation of Smad3 inhibits its transcriptional activity and antiproliferative function (*23*, *24*). There have been a number of reports on ERK phosphorylation and regulation of Smads, some of which appear to be in conflict with each other in the conclusions. The underlying mechanisms remain to be elucidated. Identification of the ERK phosphorylation sites in Smads is an essential step toward this goal.

Smad3 contains a total of nine potential ERK phosphorylation sites. Through mutational analysis, previous studies have shown that the ERK phosphorylation occurs within the four sites in the linker region. Mutation of these four sites dramatically reduces phosphorylation by ERK both in vivo and in vitro (*9*). The four potential ERK phosphorylation sites in the Smad3 linker region are Thr 178 (T178), Ser 203 (S203), Ser 207 (S207), and Ser 212 (S212). We previously briefly described that, in human HaCaT keratinocytes, ERK phosphorylated S203 and S207 and that T178 is phosphorylated more by CDK than by ERK (*23*). In this study, we characterized ERK phosphorylation of Smad3 in epithelial cells, using Mv1Lu mink lung epithelial cells as a model system. We show that EGF treatment induces a rapid phosphorylation of S207, S203, and T178. Among the ERK phosphorylation sites in Smad3, S207 is the best site. Its phosphorylation is greatly induced by EGF treatment, and it is the most sensitive site in Smad3, responding to low doses

[†] This work was supported by the National Foundation for Cancer Research, the Emerald Foundation, a Burroughs Wellcome Fund New Investigator Award, a Kimmel Scholar Award from the Sidney Kimmel Foundation for Cancer Research, and a grant from the National Institutes of Health CA93771 (to F.L.).

* Corresponding author: Fang Liu, Ph.D., Center for Advanced Biotechnology and Medicine, Rutgers University, 679 Hoes Lane, Piscataway, NJ 08854. Phone, (732)-235-5372; fax, (732)-235-4850; e-mail, fangliu@cabm.rutgers.edu.

[‡] Contributed equally to this work.

[§] Center for Advanced Biotechnology and Medicine.

[||] Susan Lehman Cullman Laboratory for Cancer Research.

[⊥] Cancer Institute of New Jersey.

[▽] Graduate Program in Molecular Biology and Biochemistry.

[1] Abbreviations: TGF-β, transforming growth factor-β; EGF, epidermal growth factor; ERK, extracellular-signal-regulated kinase; MAPK, mitogen-activated protein kinase; CDK, cyclin-dependent kinase; MBP, myelin basic protein; GAPDH, glyceraldehydes-3-phosphate dehydrogenase; PCNA, proliferating cell nuclear antigen.

10.1021/bi050560g CCC: $30.25
Published on Web 08/23/2005

of EGF. We further show that mutation of the ERK phosphorylation sites to nonphosphorylatable residues increases Smad activity to stimulate a TGF-β/Smad responsive gene, suggesting that ERK phosphorylation inhibits Smad3 activity.

MATERIALS AND METHODS

pS207, pS203, pT178, and pS212 Phosphopeptide Antibodies and Other Antibodies. Each of the phosphopeptide antibodies was raised in rabbits, affinity-purified against the phosphopeptide antigen, and cross-absorbed against the unphosphorylated peptide of the same sequence. The specificities of each of these four phosphate-specific antibodies have been demonstrated by several analyses. First, each of the phosphopeptide antibodies recognizes only the wild-type Smad3 but not the corresponding mutant Smad3 by immunoblotting (Supplementary Figure 4a in ref *23*). Second, each of the phosphopeptide antibodies can recognize overexpressed wild-type Smad3 but not the corresponding mutant form in an immunoprecipitation assay (Supplementary Figure 4b in ref *23*). Third, treatment of the phosphorylated Smad3 with a phosphatase leads to the disappearance of the phosphorylated band (Supplementary Figure 4c in ref *23*). Fourth, the band recognized by each of the phosphopeptide antibodies is Smad3, as none of these antibodies can detect a band that comigrates with Smad3 using cell extracts from Smad3$^{-/-}$ mouse embryonic fibroblasts (Supplementary Figure 4d in ref *23*). The antibodies against pERK, ATF3, and PCNA were purchased from Santa Cruz Biotechnology, Inc. The ERK antibody was from Signaling Solutions. The Smad3 antibody was from Zymed laboratories. The GAPDH antibody was from Ambion, Inc.

In Vitro Kinase Assay. Recombinant activated ERK2 MAP kinase was purchased from Calbiochem. Myelin basic protein was purchased from Sigma. The kinase reaction contains the buffer (20 mM MOPS-Na, pH 7.4, 10 mM $MgCl_2$, and 1 mM EGTA), 100 μM ATP, 3 μCi [γ-^{32}P]ATP, and appropriate amount of substrate and kinase, in a volume of 30 μL. The kinase reaction was performed at 30 °C for 30 or 20 min. The substrate titration experiments were performed under a condition that phosphate incorporation was in a linear range over the time. The reaction was terminated by addition of SDS protein gel sample buffer. Phosphorylated proteins were analyzed by SDS−PAGE followed by autoradiography. Nonradioactive kinase reactions for immunoblot analysis by phosphopeptide antibodies contained the buffer (20 mM MOPS-Na, pH 7.4, 10 mM $MgCl_2$, and 1 mM EGTA), 0.5 mM ATP, 0.3 μM GST-Smad3, and 26 ng of activated ERK2 in 30 μL. The reactions were carried out at 30 °C for 30 min.

Immunoblot Analysis. Immunoblot analyses were performed essentially as previously described (*23, 26*). In brief, cells were lysed in the TNE buffer (10 mM Tris-HCl, pH 7.8, 150 mM NaCl, and 1% NP-40) in the presence of protease and phosphatase inhibitors. Cell lysates (30 μg) were then loaded on a gel and immunoblotted by appropriate antibodies. pS207, pS203, and pT178 antibodies were used at 0.15 μg/mL. pS212 antibody was used at 0.6 μg/mL.

Transfection and Reporter Gene Assay. HepG2 cells in 60 mm dishes were transfected by DEAE−dextran and analyzed for luciferase activity as previously described (*27*). Luciferase activities were normalized by the cotransfected *Renilla* luciferase control driven by pRL-TK (Promega). Results represent the mean and standard deviation of four independent transfection experiments.

Retroviral Infection. Wild-type and each of the Smad3 phosphorylation mutants were cloned into the pLZRSΔ-IRES-GFP retroviral vector (*28*). The resulting retroviral plasmids were transfected into the ecotropic phoenix packaging cells to produce retroviruses as described previously (*29*). Mouse C2C12 myoblasts were infected with greater than 95% efficiency. At 72 h postinfection, cells were split into fresh medium. Cells were then harvested and analyzed 24 h later.

RESULTS

S207, S203, and T178 in Smad3 Are Phosphorylated by MAP Kinase in Response to EGF Treatment. Previous studies have shown that MAP kinase phosphorylation of Smad3 occurs in the linker region, within the four sites: T178, S203, S207, and S212 (*9*). We have generated phosphopeptide antibodies against each of these four sites (*23*). The specificities of each of these four phosphate-specific antibodies have been demonstrated by several analyses, including immunoblot, immunoprecipitation, phosphatase treatment, and confirming that the recognized band is Smad3 by comparing wild-type cells with Smad3 deficient cells (Supplementary Figure 4 in ref *23*).

To determine which of the four sites is phosphorylated by MAP kinase in epithelial cells, Mv1Lu mink lung epithelial cells were serum-starved overnight, treated with EGF (50 ng/mL) for 30 min, and then analyzed for Smad3 phosphorylation at these sites. As shown in Figure 1A, EGF treatment led to a rapid phosphorylation of S207, S203, and T178. We have previously shown that CDK4 and CDK2 phosphorylate T8, T178, and S212 but not S203 or S207 in vivo (*23*). Since the EGF treatment is only for 30 min, the EGF-induced phosphorylation of T178 is not due to the activation of CDK.

S207, S203, and T178 can also be phosphorylated by MAP kinase in vitro (Figure 1B). Although the S212 site can also be phosphorylated by MAP kinase in vitro (Figure 1B), we detected very little or no EGF-induced phosphorylation of endogenous S212 in vivo in either Mv1Lu epithelial cells (Figure 1B) or in HaCaT cells (*23*).

S207 Is the Best MAP Kinase Phosphorylation Site in Smad3. While S207, S203, and T178 were all phosphorylated by MAP kinase in response to EGF treatment (Figure 1A), we noticed that S207 showed the highest induction of phosphorylation by EGF in all the experiments. In addition, S207 is the only site in Smad3 that is recognized to be a MAP kinase phosphorylation site by the Scansite software program under high-stringency condition (data not shown), which recognizes a wide variety of kinase phosphorylation sites and other signature motifs. The EGF dose curve and time course experiments also confirmed this notion. As shown in Figure 1C, S207 phosphorylation was significantly induced by EGF even at a dose of 1 ng/mL. In the EGF time course experiment in Figure 1D, S207 phosphorylation was markedly increased after treatment with EGF for only 5 min, whereas significant increase in phosphorylation on the S203 or T178 occurred only after treatment for 15 min.

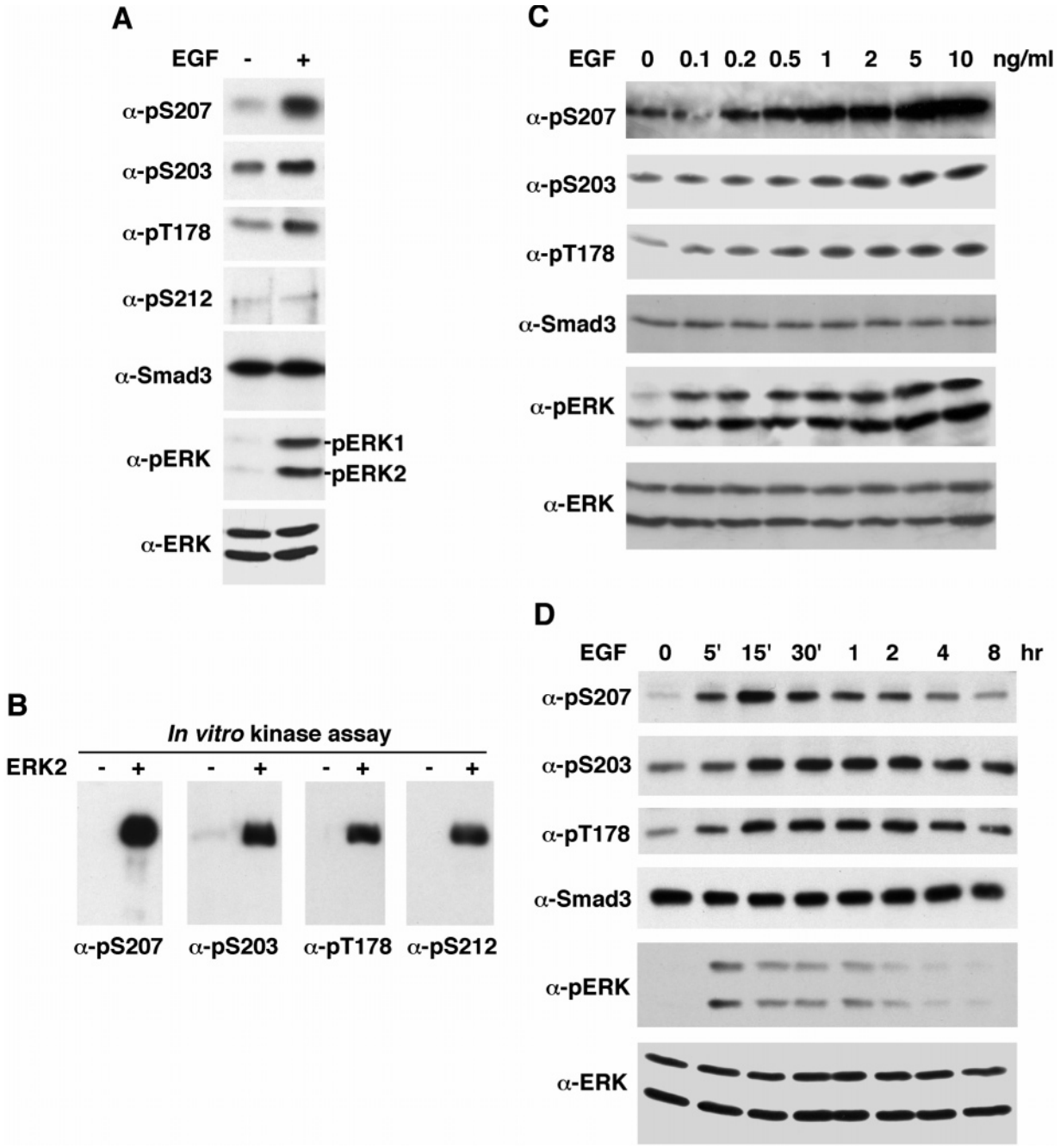

FIGURE 1: S207, S203, and T178 in Smad3 are phosphorylated by ERK in vivo and in vitro. (A) S207, S203, and T178 in Smad3 are phosphorylated in response to EGF treatment. Mv1Lu cells were serum-starved overnight and then treated with EGF (50 ng/mL) for 30 min. Cell lysates were then analyzed for the phosphorylation of S207, S203, T178, and S212 by the phosphopeptide antibodies against each of these sites in immunoblots. Smad3 expression levels, ERK activities, and ERK levels were also analyzed in immunoblots. (B) S207, S203, T178, and S212 in Smad3 can be phosphorylated by ERK2 in vitro. Twenty-six nanograms of recombinant activated ERK2 was used to phosphorylate 0.3 μM GST-Smad3 in 30 μL. The reaction products were analyzed by immunoblotting with each of the pS207, pS203, pT178, and pS212 antibodies. (C) EGF dose curve on S207, S203, and T178 phosphorylation in Smad3. Mv1Lu cells were treated with increasing concentrations of EGF as indicated for 30 min. Cell lysates were then analyzed using each of the antibodies against pS207, pS203, pT178, Smad3, pERK, and ERK. (D) EGF time course of S207, S203, and T178 phosphorylation in Smad3. Mv1Lu cells were treated with 50 ng/mL EGF for the indicated period of time. Cell lysates were then analyzed with each of the antibodies against pS207, pS203, pT178, Smad3, pERK, and ERK.

Taken together, these observations indicate that S207 is the most sensitive site in Smad3 for MAP kinase phosphorylation.

MEK Inhibitors Suppress EGF-Induced Phosphorylation of S207, S203, and T178 in Smad3. To provide further evidence that MAP kinase phosphorylates S207, S203, and T178 in response to EGF, we asked whether EGF-induced phosphorylation at these sites can be inhibited by MEK1 inhibitors. Mv1Lu cells were pretreated with MEK1 inhibitor PD98059 at 50 μM or U0126 at 3 μM for 1 h before addition of EGF. As shown in a representative experiment in Figure 2, PD 98059 and U0126 inhibited EGF-induced phosphorylation of S207, S203, and T178, confirming MAP kinase phosphorylation of these sites. The average of four experiments is plotted and presented in the lower panels of Figure 2.

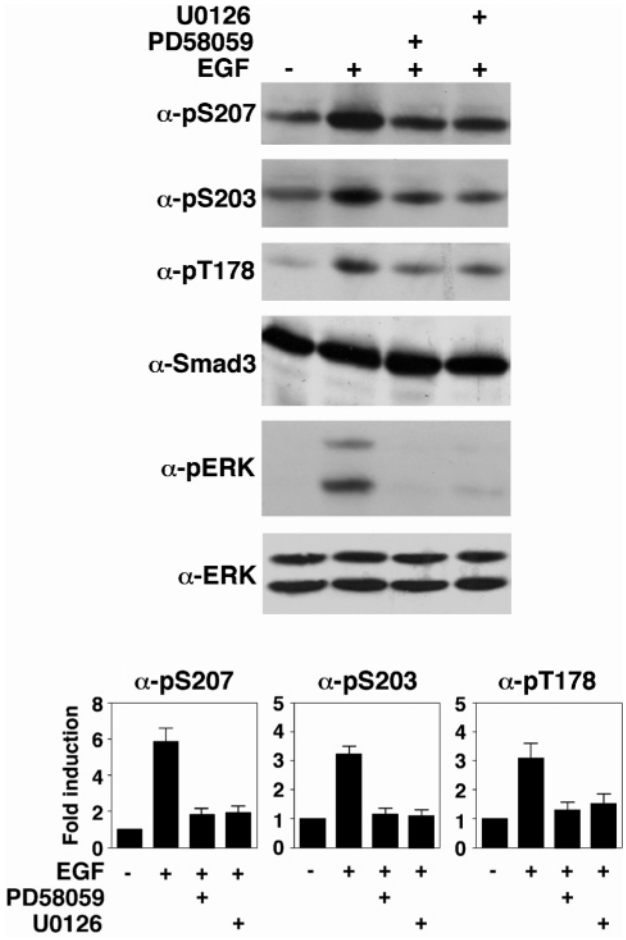

FIGURE 2: PD98059 and U0126 inhibit ERK phosphorylation of S207, S203, and T178 in Smad3. Mv1Lu cells were pretreated with 50 μM PD98059 or 3 μM U0126 for 1 h prior to the addition of EGF. Cell lysates were then analyzed for S207, S203, and T178 phosphorylation by the corresponding phosphopeptide antibodies. Smad3 level, ERK activities, and ERK levels were also analyzed as controls. One representative experiment is shown. The averages of four experiments were plotted.

Comparison of ERK2 Phosphorylation of Smad3, MBP, and Elk1 in Vitro. To determine whether Smad3 is a good substrate for ERK MAP kinase phosphorylation in vitro, we performed an in vitro kinase assay using recombinant ERK2 and GST-Smad3 as a substrate. For comparison, we also included myelin basic protein (MBP) and GST-Elk1 (307−428) as substrates in the same assay. Previous studies have shown that Elk1 is one of the best-characterized physiological substrates of ERK MAP kinase (*30, 31*), and MBP is also frequently used as a substrate to monitor ERK MAP kinase activity. Elk1 contains nine potential MAP kinase phosphorylation sites in its C-terminal domain (*30, 31*). Phosphorylation of a major site, Ser 383, is critical for Elk1 transcriptional activity (*30, 31*). Elk1 (371−428), the C-terminal domain of Elk-1, contains all the nine potential sites. Previous studies have also shown that Elk1 is a much better substrate than MBP with more than 5-fold difference in an in vitro kinase assay (*32*).

We performed an in vitro kinase assay using 1 μM substrates and increasing amount of the recombinant ERK2 (3.75, 7.5, 15, and 30 ng) at 30 °C for 30 min. Figure 3 shows both the ^{32}P gel (upper panel) and the Coomassie blue-stained gel (lower panel). As seen from the Coomassie gel,

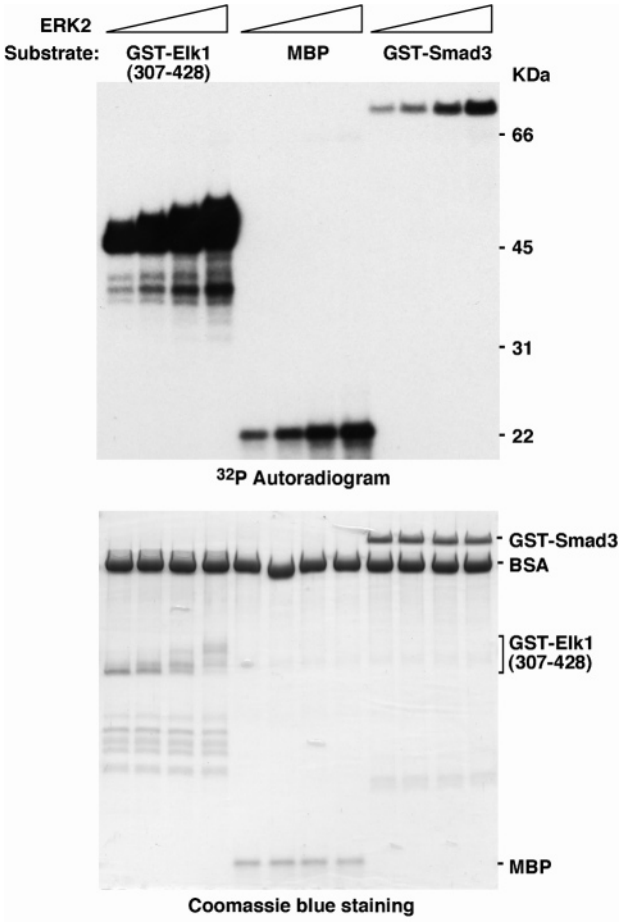

FIGURE 3: ERK2 titration for phosphorylation of Smad3, MBP, and Elk1 in vitro. One micromolar of GST-Smad3, MBP, or GST-Elk1 (307−428) was incubated with an increasing amount of recombinant activated ERK2 (3.75, 7.5, 15, and 30 ng) in the presence of γ-^{32}P-ATP at 30 °C for 30 min. The upper panel is the autoradiogram of the kinase reaction. The lower panel is the same gel stained by Coomassie blue.

Smad3 and MBP phosphorylation are in the linear range of all concentration of ERK2. The GST-Elk1 (307−428) phosphorylation led to a significant shift in migration when 7.5 ng of ERK2 was used.

To determine the kinetic parameters of ERK2 for GST-Smad3, MBP, and GST-Elk1 (307−428), we performed substrate titration experiments using 3 ng of ERK2 and an increasing amount of substrates (0.1, 0.2, 0.4, 0.8, 1.6, and 3.2 μM) at 30 °C for 20 min. Under this condition, phosphate incorporation was in a linear range over the time (data not shown). A representative ^{32}P gel is shown in Figure 4A. The phosphorylated bands were excised and counted for radioactivity, and the phosphate incorporation was plotted against substrate concentration and shown in Figure 4B. Phosphorylation of all three substrates by ERK2 follows the classic Michaelis−Menten kinetics, consistent with the previous conclusion that ERK2 phosphorylation of GST-Elk1 (307−428) and MBP obeys Michaelis−Menten kinetics (*32*). The kinetic parameters of ERK2 for GST-Smad3, MBP, and GST-Elk1 (307−428) based on three experiments are shown in Table 1. The K_m values for GST-Elk1 (307−428) and MBP are similar to those in a previous study (*32*). The ratio of V_{max} divided by K_m is a good indicator for comparing substrates. This ratio for GST-Elk1 (307−428) is significantly higher than those of MBP and Smad3. The ratio of

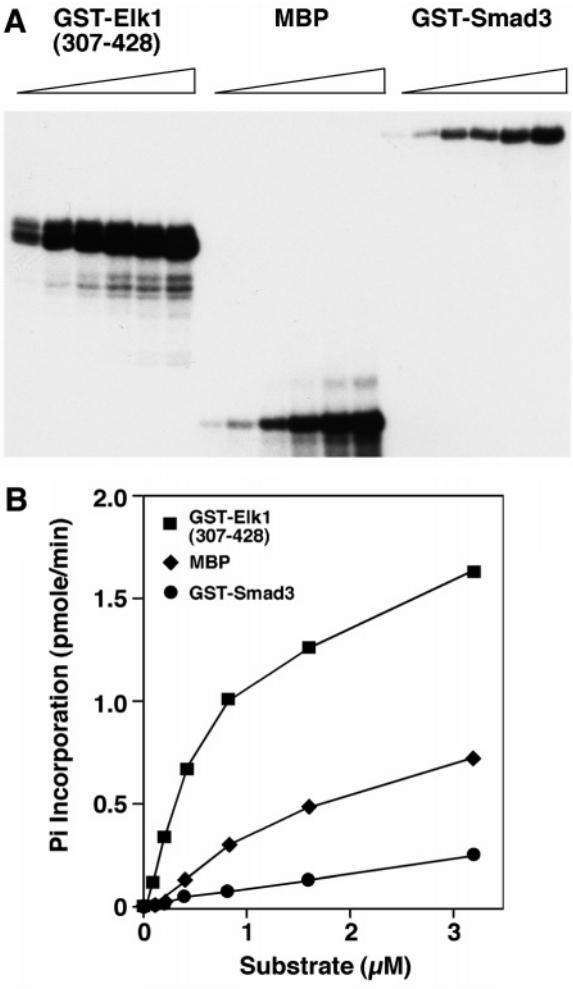

FIGURE 4: Comparison of ERK2 phosphorylation of Smad3, MBP, and Elk1 in vitro. (A) Three nanograms of ERK2 was used to phosphorylate increasing amounts of GST-Smad3, MBP, or GST-Elk1 (307−428) (0.1, 0.2, 0.4, 0.8, 1.6, and 3.2 μM) in the presence of γ-^{32}P-ATP at 30 °C for 20 min. A representative experiment is shown. (B) Phosphorylated GST-Smad3, MBP, and GST-ELK1 in panel A were excised and counted for radioactivity. The phosphate incorporation is plotted against substrate concentration.

Table 1: Kinetic Parameters of Smad3, MBP, and Elk1 for ERK2[a]

substrate	K_m[b] (μM)	V_{max}[c] (pmol/min)	V_{max}/K_m
GST-Elk1 (307−428)	1.8 ± 0.3	2.73 ± 0.60	2.27
myelin basic protein	5.1 ± 1.0	1.95 ± 0.30	0.38
GST-Smad3	11.8 ± 2.3	1.14 ± 0.19	0.10

[a] Average values from three experiments. [b] Apparent value. [c] Velocity obtained from 3 ng of recombinant ERK2.

V_{max} over K_m for Smad3 is approximately 4-fold less than that of MBP.

Analysis of the Effect of MAP Kinase Phosphorylation on Smad3 Subcellular Localization. To determine whether MAP kinase phosphorylation affects Smad3 subcellular localization, Mv1Lu cells were serum-starved overnight and then treated with EGF. Cells were harvested and fractionated into cytoplasmic and nuclear fractions. As shown in Figure 5, EGF treatment resulted in increased levels of phosphorylated S207, S203, and T178 in both the cytoplasmic and nuclear fractions. The Smad3 protein levels in the cytoplasmic fraction and the nuclear fraction remained unchanged. ERK protein levels and pERK levels were also analyzed (Figure 5), consistent with previous observations that a small proportion of activated ERK moves into the nucleus (*33*). The GAPDH (glyceraldehydes-3-phosphate dehydrogenase) served as a marker for cytoplasmic localization, whereas the PCNA (proliferating cell nuclear antigen) served as a marker for nuclear localization. The results in Figure 5 were from treatment of Mv1Lu cells with EGF for 15 min, which resulted in the highest phosphorylation of Smad3 based on the time course in Figure 1D. We also analyzed and found that treatment with EGF for 30 min or 1 h did not change the amount of Smad3 in the cytoplasmic fraction and the nuclear fraction (data not shown). These observations suggest that MAP kinase phosphorylation does not affect Smad3 localization under our experimental conditions.

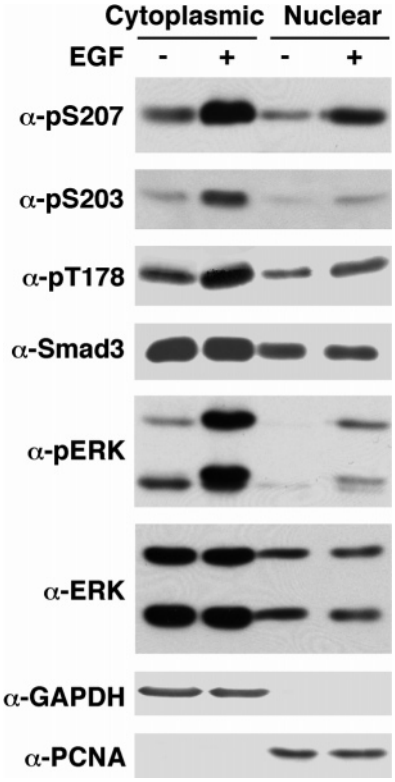

FIGURE 5: EGF treatment does not affect Smad3 subcellular localization. Mv1Lu cells were serum-starved overnight and then treated with EGF (50 ng/mL) for 15 min. Cells were then harvested and fractionated into the cytoplasmic and nuclear fractions. Approximately the same amount of total proteins were present in the cytoplasmic fraction versus the nuclear fraction. The same amount of proteins from the cytoplasmic fraction and the nuclear fraction was loaded onto SDS gels and analyzed by immunoblot for pS207, pS203, pT178, Smad3, pERK, and ERK levels. GAPDH and PCNA serve as cytoplasmic and nuclear markers, respectively.

Mutation of the MAP Kinase Phosphorylation Sites in Smad3 Increases Its Ability To Activate a Smad Target Gene. To determine the potential link between ERK MAP kinase phosphorylation and Smad3 activity, we mutated each of the three sites (T178, S203, and S207) to nonphosphorylatable residues, either individually or in combination. We then analyzed their ability to activate the A3-luciferase reporter gene, a well-characterized Smad target gene. The A3 reporter gene contains in its promoter region DNA-binding sites for Smads and for FAST-1, a winged-helix transcription factor. Smads, together with FAST-1, activate the A3 reporter gene (*5*). HepG2 cells were cotransfected with the A3-Luc reporter gene, FAST-1, and either wild-type or a phosphorylation

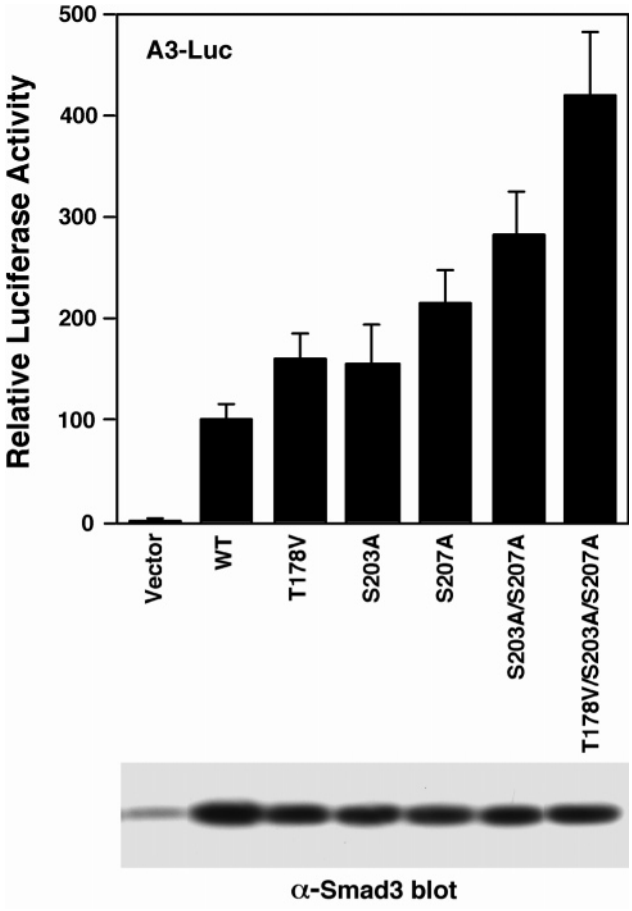

FIGURE 6: Mutation of the ERK phosphorylation sites in Smad3 increases its ability to activate a Smad reporter gene. HepG2 cells were cotransfected with the A3-Luciferase reporter gene, FAST1, and the vector control, wild-type Smad3, or a phosphorylation mutant as indicated. Luciferase activity from the average of four independent transfection experiments is shown in the upper panel. One of the transfection experiments was also analyzed for Smad3 protein expression levels as shown in the lower panel. A *t*-test was used to calculate the *P* values between wild-type Smad3 versus each of the phosphorylation mutants. The results are listed here: T178V versus wild-type Smad3, $P < 0.001$; S203A versus wild-type Smad3, $P < 0.01$; S207A versus wild-type Smad3, $P < 0.001$; S203A/S207A versus wild-type Smad3, $P < 0.001$; T178V/S203A/S207A versus wild-type Smad3, $P < 0.001$.

mutant form of Smad3. Cells were then analyzed for luciferase activity. As shown in Figure 6 (upper panel), these mutations increased the Smad3 capacity to stimulate the activity of the A3-Luc. The S207A is more active than S203A or T178V, consistent with S207 being the best MAP kinase site in Smad3. The triple mutant (T178V/S203A/S207A) and the double mutant (S203A/S207A) are more active than the single mutants in this assay. Examination of the protein levels indicated that these phosphorylation mutants were expressed at similar levels as the wild-type Smad3 as shown in Figure 6 (lower panel).

To analyze whether the phosphorylation mutants have higher activities than the wild-type Smad3 to stimulate an endogenous Smad target gene, we generated retroviruses to express the wild-type and phosphorylation mutant forms of Smad3. The retroviruses were used to infect mouse C2C12 myoblasts, which contain very low levels of endogenous Smad3. Previous studies have shown that Smad3 plays an important role to activate the expression of ATF3 as part of

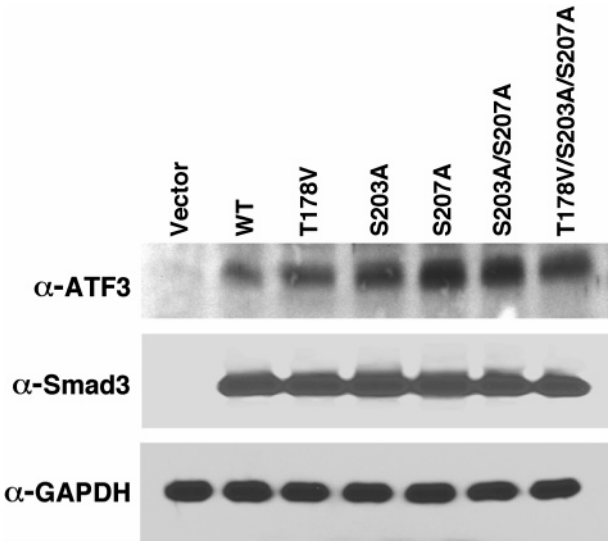

FIGURE 7: Smad3 phosphorylation mutants have increased abilities to upregulate ATF3. C2C12 cells were infected by retroviruses encoding wild-type or a phosphorylation mutant Smad3 and then analyzed by immunoblot for ATF3 levels. The expression levels of Smad3 and the GAPDH were also analyzed by immunoblot as controls.

the TGF-β/Smad antiproliferative responses (*34*). As shown in Figure 7, wild-type Smad3 activated ATF3 expression. Moreover, the phosphorylation mutant forms of Smad3 were more effective than the wild-type Smad3 at activating ATF3 expression. Taken together, these observations suggest that ERK MAP kinase phosphorylation of Smad3 inhibits its activity.

DISCUSSION

We have shown in this report that Smad3 is phosphorylated by ERK on S207, S203, and T178 in response to EGF treatment. S207 is the best ERK phosphorylation site in Smad3. Accordingly, S207 is the only site that is recognized as an ERK MAPK phosphorylation site by the Scansite program under high-stringency condition. MEK1 inhibitors PD58059 and U0126 efficiently inhibited the phosphorylation, confirming that ERK MAP kinases phosphorylate these sites in vivo. We have also compared Smad3, Elk-1, and MBP phosphorylation by recombinant activated ERK2 in vitro, and determined their kinetic parameters. Mutation of the ERK phosphorylation sites in Smad3 increases its ability to activate a Smad target gene, suggesting that ERK phosphorylation of Smad3 inhibits its activity. We have recently shown that the Smad3 linker region contains a transcriptional activation domain (*27*). Previous studies have reported that the interactions between the MAP kinase superfamily and Smad could alter signaling and transcriptional responses in either a positive or a negative manner (*8*−*22*, *35*−*44*). Future studies are warranted to determine how phosphorylation by ERK and other kinases regulate Smad3 activity in a context-dependent manner, leading to distinct biological responses.

We have also examined whether EGF treatment affects Smad3 subcellular localization. The experiments were performed in Mv1Lu cells. Because we have not found the right conditions for the phosphopeptide antibodies against pS207, pS203, or pT178 in immunofluorescence studies, we carried out the analysis via cell fractionation. Mv1Lu cells were

treated with EGF, and cell lysates were harvested and fractionated into cytoplasmic and nuclear fractions. We found that, upon EGF treatment, phosphorylated S207, S203, and T178 were increased in both the cytoplasmic and nuclear fractions, consistent with the notion that activated ERK MAP kinases are present in both the cytoplasm and the nucleus. The Smad3 protein level in the cytoplasmic fraction and the nuclear fraction remained unchanged (Figure 5). These observations suggest that ERK phosphorylation does not affect Smad3 localization under our experimental conditions. A previous study showed that the Ras−ERK pathway inhibits Smad3 nuclear accumulation (*9*). Although we could not detect appreciable changes in Smad3 subcellular localization triggered by EGF treatment in Mv1Lu cells, it remains possible that ERK phosphorylation of Smad3 can affect its subcellular localization under other conditions. The role of ERK phosphorylation on Smads subcellular localization is a complex issue. Previous studies have shown that ERK phosphorylation of Smads can inhibit, promote, or have no effect on their subcellular localization, respectively (*8*−*12*, *35*, *36*, *45*). It is possible that ERK phosphorylation of a Smad can have a different effect on its subcellular localization in a cell context-dependent manner. Future studies are necessary to identify the underlying mechanisms.

EGF can also inhibit TGF-β antiproliferative effects in a manner independent of Smad phosphorylation. For example, it has recently been shown that EGF inhibits TGF-β upregulation of p15 in primary human ovarian cancer cells and this effect is independent of phosphorylation of Smad (*45*). The mechanisms remain to be elucidated. It is speculated that TGIF, a Smad corepressor, may mediate this effect (*45*). Previous studies have shown that ERK, activated by EGF treatment, phosphorylates TGIF and stabilize it, thus, favoring the interaction between TGIF and Smad2 (*46*). The increased interaction of TGIF with Smad2 and Smad3 may contribute to the inhibition of the p15 promoter.

ERK and CDK may synergize for inhibition of Smad3 activity in a variety of biological processes as well as during tumorigenesis. We have previously shown that CDK phosphorylation inhibits Smad3 activity (*23*). CDK and ERK have distinct, as well as overlapping, phosphorylation sites. CDK phosphorylates T8, T178, and S212 (*23*), whereas ERK phosphorylates S207, S203, and T178. Their phosphorylation converges on the T178. Cancer cells often contain higher levels of ERK and CDK activities (*47*, *48*). Full inhibition of Smad3 activity by ERK and CDK together may provide an important mechanism for tumorigenesis.

ACKNOWLEDGMENT

We thank Drs. C. Abate-Shen, N. G. Ahn, M. Cobb, R. J. Davis, J. Doody, K. Guan, M. Kretzschmar, H. Lee, J. Massagué, and G. Nolan for reagents and/or suggestions and numerous colleagues for discussions.

REFERENCES

1. Roberts, A. B., and Sporn, M. B. (1990) The transforming growth factor-betas, in *Peptide Growth Factors and Their Receptors* (Sporn, M. B., and Roberts, A. B., Eds.) pp 419−472, Springer, Heidelberg, Germany.
2. Heldin, C.-H., Miyazono, K., and ten Dijke, P. (1997) TGF-β signaling from cell membrane to nucleus through SMAD proteins, *Nature 390*, 465−471.
3. Attisano, L., and Wrana, J. L. (2002) Signal transduction by the TGF-beta superfamily, *Science 296*, 1646−1647.
4. Shi, Y., and Massagué, J. (2003) Mechanisms of TGF-beta signaling from cell membrane to the nucleus, *Cell 113*, 685−700.
5. Liu, F. (2003) Receptor-regulated Smads in TGF-β signaling, *Front. Biosci. 8*, S1280−1303.
6. Derynck, R., and Zhang, Y. E. (2003) Smad-dependent and Smad-independent pathways in TGF-beta family signalling, *Nature 425*, 577−584.
7. ten Dijke, P., and Hill, C. S. (2004) New insights into TGF-beta-Smad signaling, *Trends Biochem. Sci. 29*, 265−273.
8. Kretzschmar, M., Doody, J., and Massague J. (1997) Opposing BMP and EGF signalling pathways converge on the TGF-beta family mediator Smad1, *Nature 389*, 618−622.
9. Kretzschmar, M., Doody, J., Timokhina, I., and Massague, J. (1999) A mechanism of repression of TGF-beta/Smad signaling by oncogenic ras, *Genes Dev. 13*, 804−816.
10. Grimm, O. H., and Gurdon, J. B. (2002) Nuclear exclusion of Smad2 is a mechanism leading to loss of competence, *Nat. Cell Biol. 4*, 519−522.
11. de Caestecker, M. P., Parks, W. T., Frank, C. J., Castagnino, P., Bottaro, D. P., Roberts, A. B., and Lechleider, R. J. (1998) Smad2 transduces common signals from receptor serine-threonine and tyrosine kinases, *Genes Dev. 12*, 1587−1592.
12. Blanchette, F., Rivard, N., Rudd, P., Grondin, F., Attisano, L., and Dubois, C. M. (2001) Cross-talk between the p42/p44 MAP kinase and Smad pathways in transforming growth factor beta 1-induced furin gene transactivation, *J. Biol. Chem. 276*, 33986−33994.
13. Funaba, M., Zimmerman, C. M., and Mathews, L. S. (2002) Modulation of Smad2-mediated signaling by extracellular signal-regulated kinase, *J. Biol. Chem. 277*, 41361−41368.
14. Sater, A. K., El-Hodiri, H. M., Goswami, M., Alexander, T. B., Al-Sheikh, O., Etkin, L. D., and Akif Uzman, J. (2003) Evidence for antagonism of BMP-4 signals by MAP kinase during *Xenopus* axis determination and neural specification, *Differentiation 71*, 434−444.
15. Pera, E. M., Ikeda, A., Eivers, E., and De Robertis, E. M. (2003) Integration of IGF, FGF, and anti-BMP signals via Smad1 phosphorylation in neural induction, *Genes Dev. 17*, 3023−3028.
16. Massagué, J. (2003) Integration of Smad and MAPK pathways: a link and a linker revisited, *Genes Dev. 17*, 2993−2997.
17. Aubin, J., Davy, A., and Soriano, P. (2004) In vivo convergence of BMP and MAPK signaling pathways: impact of differential Smad1 phosphorylation on development and homeostasis, *Genes Dev. 18*, 1482−1494.
18. De Robertis, E. M., and Kuroda, H. (2004) Dorsal−ventral patterning and neural induction in *Xenopus* embryos, *Annu. Rev. Cell Dev. Biol. 20*, 285−308.
19. Engel, M. E., McDonnell, M. A., Law, B. K., and Moses, H. L. (1999) Interdependent SMAD and JNK signaling in transforming growth factor-beta-mediated transcription, *J. Biol. Chem. 274*, 37413−37420.
20. Mori, S., Matsuzaki, K., Yoshida, K., Furukawa, F., Tahashi, Y., Yamagata, H., Sekimoto, G., Seki, T., Matsui, H., Nishizawa, M., Fujisawa, J., and Okazaki, K. (2004) TGF-beta and HGF transmit the signals through JNK-dependent Smad2/3 phosphorylation at the linker regions, *Oncogene 23*, 7416−742.
21. Furukawa, F., Matsuzaki, K., Mori, S., Tahashi, Y., Yoshida, K., Sugano, Y., Yamagata, H., Matsushita, M., Seki, T., Inagaki, Y., Nishizawa, M., Fujisawa, J., and Inoue, K. (2003) p38 MAPK mediates fibrogenic signal through Smad3 phosphorylation in rat myofibroblasts, *Hepatology 38*, 879−889.
22. Kamaraju, A. K., and Roberts, A. B. (2005) Role of Rho/ROCK and p38 MAP kinase pathways in TGF-beta-mediated Smad-dependent growth inhibition of human breast carcinoma cells in vivo, *J. Biol. Chem. 280*, 1024−1036.
23. Matsuura, I., Denissova, N. G., Wang, G., He, D., Long, J., and Liu, F. (2004) Cyclin-dependent kinases regulate the antiproliferative function of Smads, *Nature 430*, 226−231.
24. Liu, F., and Matsuura, I. (2005) Inhibition of Smad antiproliferative function by CDK phosphorylation, *Cell Cycle 4*, 63−66.
25. Wicks, S. J., Lui, S., Abdel-Wahab, N., Mason, R. M., and Chantry. A. (2000) Inactivation of Smad-transforming growth factor beta signaling by Ca(2+)-calmodulin-dependent protein kinase II, *Mol. Cell. Biol. 20*, 8103−8111.

26. Long, J., Wang, G., Matsuura, I., He, D., and Liu, F. (2004) Activation of Smad transcriptional activity by protein inhibitor of activated STAT3 (PIAS3), *Proc. Natl. Acad. Sci. U.S.A. 101*, 99−104.
27. Wang, G., Long, J., Matsuura, I., He, D., and Liu, F. (2005) The Smad3 linker region contains a transcriptional activation domain, *Biochem. J. 386*, 29−34.
28. Kim, M. J. Bhatia-Gaur, R., Banach-Petrosky, W. A., Desai, N., Wang, Y., Hayward, S. W., Cunha, G. R., Cardiff, R. D., Shen, M. M., and Abate-Shen, C. (2002) *Nkx3.1* mutant mice recapitulate early stages of prostate carcinogenesis, *Cancer Res. 62*, 2999−3004.
29. Swift, S., Lorens, J., Achacoso, P., and Nolan, G. P. (1999) Rapid production of retroviruses for efficient gene delivery to mammalian cells using 293T cell-based systems, in *Current Protocols in Immunology* (Coligan, J. E., et al., Eds.) pp 10.17.14−10.17.29, John Wiley & Sons, New York.
30. Marais, R., Wynne, J., and Treisman, R. (1993) The SRF accessory protein Elk-1 contains a growth factor-regulated transcriptional activation domain, *Cell 73*, 381−393.
31. Hill, C. S., and Treisman, R. (1995) Transcriptional regulation by extracellular signals: mechanisms and specificity, *Cell 80*, 199−211.
32. Zhou, B., and Zhang, Z. Y. (2002) The activity of the extracellular signal-regulated kinase 2 is regulated by differential phosphorylation in the activation loop, *J. Biol. Chem. 277*, 13889−13899.
33. Blenis, J. (1993) Signal transduction via the MAP kinases: proceed at your own RSK, *Proc. Natl. Acad. Sci. U.S.A. 90*, 5889−5892.
34. Kang, Y., Chen, C. R., and Massague, J. (2003) A self-enabling TGFbeta response coupled to stress signaling: Smad engages stress response factor ATF3 for Id1 repression in epithelial cells, *Mol. Cell 11*, 915−926.
35. Hu, P. P, Shen, X., Huang, D., Liu, Y., Counter, C., and Wang X.-F. (1999) The MEK pathway is required for stimulation of p21(WAF1/CIP1) by transforming growth factor-beta, *J. Biol. Chem. 274*, 35381−35387.
36. Lehmann, K., Janda, E., Pierreux, C. E., Rytomaa, M., Schulze, A., McMahon, M., Hill, C. S., Beug, H., and Downward, J. (2000) Raf induces TGFbeta production while blocking its apoptotic but not invasive responses: a mechanism leading to increased malignancy in epithelial cells, *Genes Dev. 14*, 2610−2622.
37. Brown, J. D., DiChiara, M. R., Anderson, K. R., Gimbrone, M. A., Jr., and Topper, J. N. (1999) MEKK-1, a component of the stress (stress-activated protein kinase/c-Jun N-terminal kinase) pathway, can selectively activate Smad2-mediated transcriptional activation in endothelial cells, *J. Biol. Chem. 274*, 8797−8805.
38. Yue, J., and Mulder, K. M. (2000) Requirement of Ras/MAPK pathway activation by transforming growth factor beta for transforming growth factor beta 1 production in a Smad-dependent pathway, *J. Biol. Chem. 275*, 30765−30773.
39. Mulder, K. M. (2000) Role of Ras and Mapks in TGFbeta signaling, *Cytokine Growth Factor Rev. 11*, 23−35.
40. Yue, J., Sun, B., Liu, G., and Mulder, K. M. (2004) Requirement of TGF-beta receptor-dependent activation of c-Jun N-terminal kinases (JNKs)/stress-activated protein kinases (Sapks) for TGF-beta up-regulation of the urokinase-type plasminogen activator receptor, *J. Cell. Physiol. 199*, 284−292.
41. Ventura, J. J., Kennedy, N. J., Flavell, R. A., and Davis, R. J. (2004) JNK regulates autocrine expression of TGF-beta1, *Mol. Cell 15*, 269−278.
42. Pardoux, C., and Derynck, R. (2004) JNK regulates expression and autocrine signaling of TGF-beta1, *Mol. Cell 15*, 170−171.
43. Hayes, S. A., Huang, X., Kambhampati, S., Platanias, L. C., and Bergan, R. C. (2003) p38 MAP kinase modulates Smad-dependent changes in human prostate cell adhesion, *Oncogene 22*, 4841−4850.
44. Hayashida, T., Decaestecker, M., and Schnaper, H. W. (2003) Cross-talk between ERK MAP kinase and Smad signaling pathways enhances TGF-beta-dependent responses in human mesangial cells, *FASEB J. 17*, 1576−1578.
45. Dunfield, L. D, and Nachtigal, M. W. (2003) Inhibition of the antiproliferative effect of TGFbeta by EGF in primary human ovarian cancer cells, *Oncogene 22*, 4745−4751.
46. Lo, R. S., Wotton, D., and Massague J. (2001) Epidermal growth factor signaling via Ras controls the Smad transcriptional co-repressor TGIF, *EMBO J. 20*, 128−136.
47. McCormick, F. (1999) Signalling networks that cause cancer, *Trends Cell Biol. 9*, M53−M56.
48. Sherr, C. J., and McCormick, F. (2002) The RB and p53 pathways in cancer, *Cancer Cell 2*, 103−112.

BI050560G